Density Functional Calculations

Two Faces of a Biomimetic Non-Heme HO–Fe^{V}=O Oxidant: Olefin Epoxidation versus *cis*-Dihydroxylation**

Arianna Bassan, Margareta R. A. Blomberg, Per E. M. Siegbahn, and Lawrence Que, Jr.**

The family of non-heme iron complexes—exemplified by $[Fe^{II}(tpa)(CH_3CN)_2]^{2+}$, where tpa is the tetradentate tripodal tris(2-pyridylmethyl)amine ligand—efficiently utilizes H_2O_2 to carry out stereospecific olefin epoxidation and *cis*-dihydroxylation.[1–4] The latter reaction was not previously known to be catalyzed by a synthetic iron complex and is precedented only in the chemistry of Rieske dioxygenases,[5] non-heme iron enzymes responsible for *cis*-dihydroxylation in the biodegradation of arenes by soil bacteria. Isotope-labeling experiments on the biomimetic reaction show the involvement of a highly selective metal-based oxidant capable of introducing water into the product.[1,2] This oxidant is proposed to result from the low-spin complex $[Fe^{III}(tpa)(H_2●)(OOH)]^{2+}$ (**1**) and be a formally H●–Fe^{V}=O species (**2**; ● indicates an oxygen atom with isotope labeling), both shown in Figure 1.

Previous DFT calculations have demonstrated the feasibility of an O–O bond heterolysis mechanism that leads to an $S = 3/2$ *cis*-HO–Fe^{V}=O species with a short Fe–O bond (1.66 Å) and a longer Fe–OH bond (1.77 Å).[6] The three unpaired electrons are mainly distributed on the iron atom (1.58), the oxo oxygen atom (1.0), and the hydroxo oxygen atom (0.44): a spin distribution not unlike that found for compounds I of heme peroxidases and cytochrome P450 and related model complexes.[7,8] The corresponding sextet and doublet states of HO–Fe^{V}=O lie more than 10 kcal mol^{-1} higher in energy than the quartet ground state.[9]

Further DFT calculations presented herein provide new insight into how this unique oxidant can carry out both olefin epoxidation and *cis*-dihydroxylation. Hence, the present study focuses on the subsequent reaction of **2** with olefins (see the Supporting Information) to reveal that olefin epoxidation and *cis*-dihydroxylation in fact represent different faces of the same oxidant.

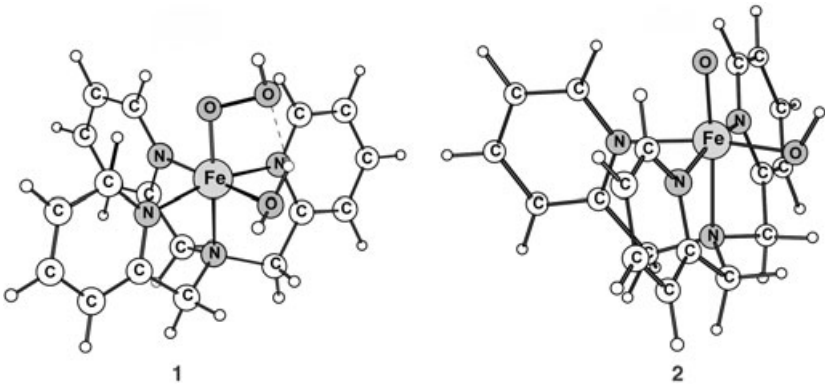

Figure 1. Structures of the $[Fe^{III}(tpa)(H_2O)(OOH)]^{2+}$ precursor (**1**) and the proposed metal-based *cis*-HO–Fe^{V}=O oxidant (**2**).

The key results of our DFT study are illustrated by the energy profiles in Figure 2, showing that **2** can react with olefins (namely, 2-butene) through two different channels. As shown on the left, the oxo group attacks the olefin to form the C1–O1 bond and intermediate **A**-Fe^{IV} (path A). On the right, the hydroxo ligand attacks the olefin to form the C2–O2 bond and intermediate **B**-Fe^{IV} (path B). Both intermediates have an iron(IV) center and a radical on the partially oxidized substrate.

Intermediate **A**-Fe^{IV} is an iron(IV) complex with a hydroxide ($r_{Fe-O2} = 1.79$ Å) and the partially oxidized olefin as ligands. The formation of the new C1–O1 bond is exergonic by 2.5 kcal mol^{-1} and involves an activation energy of 7.8 kcal mol^{-1}; solvent effects (+3.1 kcal mol^{-1}), entropy effects (+0.6 kcal mol^{-1}), and big-basis effects (+2.1 kcal mol^{-1}) contribute to increase the barrier by 5.6 kcal mol^{-1}. Unpaired spin density can be found on the metal center (1.53), the partially oxidized olefin (0.97), and the remaining ligands (0.50). Antiferromagnetic coupling of the unpaired electron on the partially oxidized olefin with those of the metal center affords an $S = 1/2$ state that is more stable by about 1–2 kcal mol^{-1} than the corresponding $S = 3/2$ state. Thus, a spin crossing between the quartet and the doublet surfaces may occur in the vicinity of this intermediate during the course of epoxidation. Intermediate **A**-Fe^{IV} in the $S = 1/2$ state decays spontaneously and without any significant barrier to the epoxide in the first coordination sphere of iron. No low-energy pathway producing the *cis*-diol from **A**-Fe^{IV} can be found. Almost identical barriers were obtained when epoxidation of propene was investigated.

In contrast, *cis*-dihydroxylation of the olefin occurs when the hydroxo ligand of **2** attacks the substrate, thus leading to

[*] Dr. A. Bassan, Prof. M. R. A. Blomberg, Prof. P. E. M. Siegbahn
Department of Physics
Stockholm University
SE 106 91, Stockholm (Sweden)
Fax: (+46) 8-5537-8601
E-mail: arianna@physto.se
Prof. L. Que, Jr.
Department of Chemistry and
Center for Metals in Biocatalysis
University of Minnesota
Minneapolis, MN 55455 (USA)
Fax: (+1) 612-624-7029
E-mail: que@chem.umn.edu

[**] The bio-inspired catalysis work at the University of Minnesota is supported by the US Department of Energy (grant no. DE-FG02-03ER15455 to L.Q.). We gratefully acknowledge the National Supercomputer Center (Sweden) for generous grants of computer time. We thank Dr. Megumi Fujita for useful discussions.

Supporting information for this article is available on the WWW under http://www.angewandte.org or from the author.

 DOI: 10.1002/ange.200463072

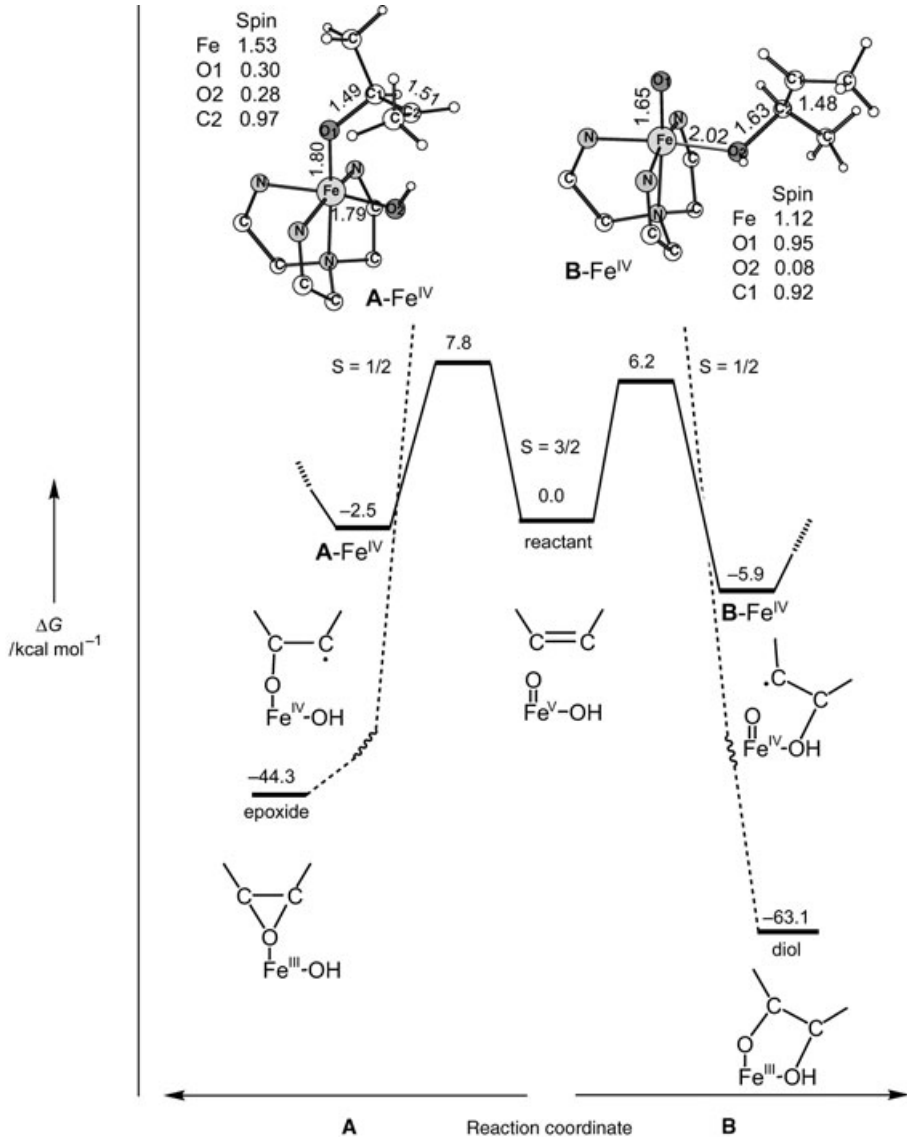

Figure 2. Energy profiles for olefin epoxidation (path A) and olefin *cis*-dihydroxylation (path B).

the formation of intermediate **B**-Fe^{IV}. The Fe=O double bond is maintained ($r_{Fe\text{-}O1} = 1.65$ Å) in this species and a weak C2–O2 bond ($r_{C2\text{-}O2} = 1.63$ Å) is formed. For the $S = 3/2$ state of **B**-Fe^{IV}, unpaired spin density can be found on the metal center (1.12), the oxo oxygen atom (0.95), and the partially oxidized olefin (0.97). The transition state for C2–O2 bond formation in propene was found to have an energy barrier of 6.2 kcal mol^{-1}, a value which includes solvent effects (2.2 kcal mol^{-1}), big-basis effects (1.5 kcal mol^{-1}), and thermal and zero-point corrections (0.6 kcal mol^{-1}). In the case of butene, the corresponding transition-state structure could not be optimized but is approximated to have a relative energy similar to that of the propene complex. As with the epoxidation pathway, a spin crossing from the quartet to the doublet state of **B**-Fe^{IV} results in the formation of the product, because the $S = 1/2$ state readily leads to the diol without any significant energy barrier. In line with the chemistry of other transition metal oxides, for example, osmium tetroxide,[10] the concerted [3+2] addition of HO–Fe=O across the olefin C=C bond was also probed, but all attempts to optimize the corresponding structure led to a transition state where only one C–O bond was initially formed.

We also considered the possibility that *cis*-diol is produced from the initially formed epoxide. Figure 3 shows the calculated energy profile for this conversion for the $S = 5/2$ state, which is the ground state for both products (see the Supporting Information). Figure 3 also reports the energy required for epoxide dissociation from the metal center. Interestingly the epoxide-to-diol conversion is disfavored relative to epoxide release from the metal center by approximately 7 kcal mol^{-1}. Thus, diol formation most likely occurs by the direct reaction of olefin with the HO–Fe^{V}=O species, rather than via the epoxide.

The Fe(tpa) family of complexes are unique oxidation catalysts that are capable of both olefin epoxidation and *cis*-dihydroxylation.[4] As previously suggested,[1,2,6] it is likely that a high-valent iron–oxo species is formed along the reaction pathway, and our DFT calculations have provided insight into the mechanism of olefin oxidation by the exceptional HO–Fe^{V}=O oxidant. It is possible that epoxidation may also occur by direct attack of the precursor Fe–OOH on the olefin, and a preliminary study in this direction has suggested that such a pathway is slightly disfavored over the competing O–O bond cleavage to generate the HO–Fe^{V}=O oxidant.

If the Fe(tpa) catalysts carry out olefin oxidation via the high-valent iro–oxo species, then epoxidation occurs by attack of the oxo oxygen atom on the olefin, and *cis*-dihydroxylation is initiated by attack of the hydroxo oxygen atom, followed by rebound of the incipient carbon radical with the oxo oxygen atom. This scheme provides a rationale for the observed incorporation of one oxygen atom from H_2O_2 and one oxygen atom from solvent into the diol product.[2] Such a mechanism may also explain why the oxygen atom of the epoxide derives principally, but not exclusively, from H_2O_2. Previous DFT calculations have determined that oxo–hydroxo tautomerization of the H●–Fe^{V}=O species leading to label scrambling has an energy barrier of about 10 kcal mol^{-1},[9] a value that is somewhat higher than that computed here for olefin epoxidation, so oxo attack on the olefin would be expected to occur before significant label scrambling occurs, in agreement with experimental observations.

Lastly, the calculations reveal that olefin epoxidation and *cis*-dihydroxylation have comparable activation barriers, with the latter being favored by about 1 kcal mol^{-1} (Figure 2). On the basis of transition-state theory, this difference predicts a diol-to-epoxide ratio of about 5:1. Experimentally, the *cis*-diol

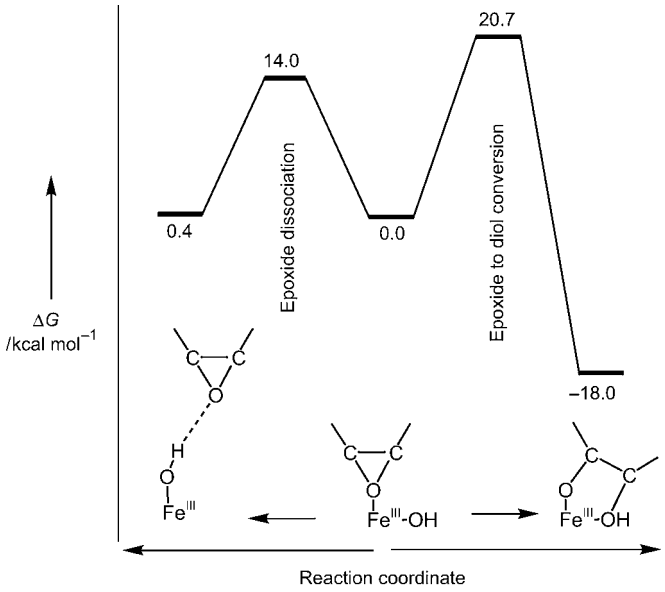

Figure 3. Energy profiles for epoxide dissociation and epoxide-to-diol conversion for the $S = 5/2$ state.

product is indeed favored over the epoxide, but only by factors of 1.2–3, depending on the olefin, results well within the accuracy of the present computational approach.

These new insights, only obtainable from DFT calculations thus far, provide a solid foundation for understanding the reaction mechanisms of a new family of bio-inspired non-heme iron catalysts for olefin oxidation. The stage has thus been set for future work aimed at rationalizing the strong preference for epoxide products by related Fe(bpmen) and α-Fe(bpmcn) catalysts[11] as well as the exclusive production of *cis*-diol product in the oxidation of electron-deficient olefins like acrylate and fumarate by the Fe(tpa) catalyst.[12]

Methods

The energy profiles and the structures included in the present study were obtained employing the B3LYP functional and using the quantum chemical programs Jaguar 4.2[13] and Gaussian 98.[14] Fully optimized transition states were obtained through the evaluation of the second derivatives with respect to the nuclear coordinates of approximate structures. Hessians for reactants, intermediates, and transition states were used to derive the zero-point effects and the thermal corrections necessary for determining Gibbs free energies. Free energies are reported including zero point and thermal effects, evaluated for 298.15 K. Relative free energies for epoxidation and *cis*-dihydroxylation were calculated with a supermolecular approach including both the metal complex and the olefin (see, for example, Figure S1 in the Supporting Information). This is likely to underestimate the energy barriers but does not affect the conclusions of this study.

An effective core potential was used to describe the iron atom. In the geometry optimizations and in the Hessian evaluations all the other atoms were described by a standard double zeta basis set, labeled lacvp in Jaguar. The final B3LYP energies for the fully optimized structures were computed using a basis set that includes polarization functions on all atoms (labeled lacv3p** in Jaguar). Spin populations obtained with the lacvp basis set are reported. Solvent effects were evaluated employing the self-consistent reaction field as implemented in Jaguar[13] together with a dielectric constant of 36.64 and a probe radius of 2.155 Å.

On the basis of previous benchmarks, an accuracy of about 3–5 kcal mol^{-1} could affect the energy profiles reported in the present investigation.[15,16] However, such an accuracy should be enough to discriminate among different reaction mechanisms.

Received: December 27, 2004

Keywords: density functional calculations · dihydroxylation · enzyme models · epoxidation · iron

[1] K. Chen, L. Que, Jr., *J. Am. Chem. Soc.* **2001**, *123*, 6327–6337.
[2] K. Chen, M. Costas, J. Kim, A. K. Tipton, L. Que, Jr., *J. Am. Chem. Soc.* **2002**, *124*, 3026–3035.
[3] K. Chen, M. Costas, L. Que, Jr., *J. Chem. Soc. Dalton Trans.* **2002**, *5*, 672–679.
[4] M. Costas, M. P. Mehn, M. P. Jensen, L. Que, Jr., *Chem. Rev.* **2004**, *104*, 159–172.
[5] D. T. Gibson, R. E. Parales, *Curr. Opin. Biotechnol.* **2002**, *13*, 235–243.
[6] A. Bassan, M. R. A. Blomberg, P. E. M. Siegbahn, L. Que, Jr., *J. Am. Chem. Soc.* **2002**, *124*, 11056–11063.
[7] G. H. Loew, D. Harris, *Chem. Rev.* **2000**, *100*, 407–419.
[8] S. Shaik, S. P. de Visser, F. Ogliaro, H. Schwarz, D. Schröder, *Curr. Opin. Chem. Biol.* **2002**, *6*, 556–557.
[9] A. Bassan, M. R. A. Blomberg, P. E. M. Siegbahn, L. Que, Jr., *Chem. Eur. J.* **2004**, *11*, 692–705.
[10] D. V. Deubel, G. Frenking, *Acc. Chem. Res.* **2003**, *36*, 645–651.
[11] M. Costas, L. Que, Jr., *Angew. Chem. Int. Ed.* **2002**, *41*, 2179–2181 (bpmen = *N*,*N*′-bis(2-pyridylmethyl)-*N*,*N*′-dimethyl-1,2-diaminoethane, bpmcn = *N*,*N*′-bis(2-pyridylmethyl)-*N*,*N*′-dimethyl-*trans*-1,2-diaminocyclohexane.
[12] M. Fujita, M. Costas, L. Que, Jr., *J. Am. Chem. Soc.* **2003**, *125*, 9912–9913.
[13] JAGUAR 4.2, Schrödinger, Inc., Portland, Oregon, **2000**; see: G. Vacek, J. K. Perry, J.-M. Langlois, *Chem. Phys. Lett.* **1999**, *310*, 189–194.
[14] Gaussian 98 (Revision A.7), M. J. Frisch, G. W. Trucks, H. B. Schlegel, G. E. Scuseria, M. A. Robb, J. R. Cheeseman, V. G. Zakrzewski, J. A. Montgomery, R. E. Stratmann, J. C. Burant, S. Dapprich, J. M. Millam, A. D. Daniels, K. N. Kudin, M. C. Strain, O. Farkas, J. Tomasi, V. Barone, M. Cossi, R. Cammi, B. Mennucci, C. Pomelli, C. Adamo, S. Clifford, J. Ochterski, G. A. Petersson, P. Y. Ayala, Q. Cui, K. Morokuma, D. K. Malick, A. D. Rabuck, K. Raghavachari, J. B. Foresman, J. Cioslowski, J. V. Ortiz, B. B. Stefanov, G. Liu, A. Liashenko, P. Piskorz, I. Komaromi, R. Gomperts, R. L. Martin, D. J. Fox, T. Keith, M. A. Al-Laham, C. Y. Peng, A. Nanayakkara, C. Gonzalez, M. Challacombe, P. M. W. Gill, B. G. Johnson, W. Chen, M. W. Wong, J. L. Andres, M. Head-Gordon, E. S. Replogle, J. A. Pople, Gaussian, Inc., Pittsburgh, PA, **1998**.
[15] M. R. A. Blomberg, P. E. M. Siegbahn in *Transition State Modeling for Catalysis* (Eds: D. G. Truhlar, K. Morokuma), American Chemical Society, Washington DC, **1999**, pp. 49–60.
[16] P. E. M. Siegbahn, *J. Comput. Chem.* **2001**, *22*, 1634–1645.

